Visually Induced Motion Sickness Estimation and Prediction in Virtual Reality using Frequency Components Analysis of Postural Sway Signal

J.-R. Chardonnet[1], M. A. Mirzaei[1] and F. Mérienne[1]

[1]LE2I UMR6306, Arts et Métiers, CNRS, Univ. Bourgogne Franche-Comté, HeSam, France

Abstract

The paper proposes a method for estimating and predicting visually induced motion sickness (VIMS) occurring in a navigation task in a 3D immersive virtual environment, by extracting features from the body postural sway signals in both the time and frequency domains. Past research showed that the change in the body postural sway may be an element for characterizing VIMS. Therefore, we conducted experiments in a 3D virtual environment where the task was simply a translational movement with different navigation speeds. By measuring the evolution of the body's center of gravity (COG), the analysis of the sway signals in the time domain showed a dilation of the COG's area, as well as a change in the shape of the area. Frequency Components Analysis (FCA) of the sway signal gave an efficient feature to estimate and predict the level of VIMS. The results provide promising insight to better monitor sickness in a virtual reality application.

Categories and Subject Descriptors (according to ACM CCS): H.1.2 [Models and principles]: User/Machine Systems—Human information processing H.5.1 [Information Interfaces and Presentation]: Multimedia Information Systems—Artificial, augmented, and virtual realities H.5.2 [Information Interfaces and Presentation]: User interfaces—Evaluation/methodology

1. Introduction

When humans are exposed to motion (for instance, in a car or a train), they may get sick. This may be due to physical self-motion, motion of the visual scene alone, or a combination of both. Typically, the sickness induced by synthetic conditions, like being on a moving platform, is called motion sickness (MS), while the one induced by viewing visual motion (as stationary observers) is called visually induced motion sickness (VIMS) in the literature. Virtual reality (VR) faces the same issue as a user can be exposed to visual motion while navigating in a 3D immersive virtual environment (VE) (for instance during navigation in a scale-one virtual building for project reviews purposes, which is a major application of this work).

This paper aims at studying VIMS occurring in a typical navigation task in VR by considering the upright postural stance sway in both the time and frequency domains, in addition to well-known subjective studies. This will allow us to point out some features which will explain and predict VIMS in terms of frequency components.

1.1. Related work

Human experience with MS dates back to the time when US Admiral Nelson reported his soldiers were suffering from boat sickness [Mon72]. He found out by experience that adaptation and repeated exposure can minimize these adverse effects. Additionally, humans encountering with motion and virtual environments demonstrate that MS adversely affects susceptible individuals [Ben88]. Indeed people without functioning organs of balance in the inner ears, so called labyrinthine defectives, never get sick from motion [Irw81, KGMB68]. Interestingly, these patients do not suffer also from visual motion, even in the absence of physical self-motion [CHM91]. Another work showed that passive passengers get sicker than active people, i.e., people controlling their motion themselves [SH98]. Reason and Brand [RB75] suggested a theory on motion sickness, the so-called "sensory conflict theory". They accordingly stated that "*motion sickness is a self-inflicted maladaptation phenomenon which occurs at the onset and cessation of conditions of sensory rearrangement when the pattern of in-*

puts from the vestibular system, other proprioceptors and vision is at variance with the stored patterns derived from recent transactions with the spatial environment". Though the theory was very successful in explaining many of previously observed phenomena, it also had some flaws. Bos et al. further detailed this theory focusing on the observation that "*people only get sick when there is an (apparent) change of gravity with respect to their head*" [BBG08].

In VR, it is well-known that immersive systems are prone to generate sickness (see for example [Kol95] for a pioneering study on the topics).

MS and VIMS can be measured by psychological and physiological means, among which the simulator sickness questionnaire (SSQ) is a well-known psychological method for measuring the extent of MS [KLBL93]. Physiological methods include blood pressure, electrogastrography, heart rate variability (e.g., [YAM*05]) and human postural sway [TFMM07].

Focusing on the body postural sway, past studies suggest that animals experience sickness symptoms in circumstances where they have not acquired strategies to maintain their balance, meaning MS is caused by postural instability [SSBP99]. It has also been reported that the onset of motion sickness may be preceded by significant increases of the postural sway [SHH*00]. A projection of a body's center of gravity (COG) on a detection balance board can be measured as an average of the center of pressure (COP) of both feet. The analysis of the COG signal gives a good insight into the control theory of two-legged robots and the human stance [Tah09]. Body balance malfunctions when exposing to 3D visual stimuli [TFMM07]. Several parameters such as the area of sway, the total locus length and the locus length per unit area have been widely proposed in clinical studies to quantify the instability involved in the standing posture [OTS*95]. It has been reported that a wide stance significantly increases the total locus length of the COG of individuals with high SSQ scores; while the length in those of individuals with low scores is less affected by such a stance [SVBS07]. Takada et al. observed that the density of the COP decreases during exposure to stereoscopic images, i.e., the COG changes from a dense distribution to a sparse one [TFMM07]. They notice that the sparse density and the dilation of the COG area would be useful indexes to measure VIMS. Postural stability as a measure for sickness has been studied also in VR for a long time, e.g., [Cob99, KS96], but most of the studies have been considering only the COG's locus length and were conducted using either head-mounted displays (HMD), either large screens.

1.2. Contribution

This paper's contribution lies in the use of frequency components analysis of the body postural sway to estimate and predict VIMS occurrence and the level of sickness in a typical navigation task in a 3D immersive VE. Not only the COG's projection area will be measured (mostly considered in past research), but its shape will also be used as features to explain VIMS. We will prove the following two hypotheses:

(H1) the COG's area starts dilating, its geometric shape tends to change from an ellipse to a circle when VIMS appears, and though with a constant speed sickness may occur easily, the navigation speed is increased to ensure strong area density and shape changes;

(H2) the frequency components of the COG signal's spectrum split into two parts, and the second part (corresponding to involuntary movements) moves away from the first one (corresponding to voluntary movements) when sickness appears and increases.

Since the COG's area, shape and frequency components are pointing at the same signal, they are correlated.

The paper is organized as follows: Section 2 briefly explains the theory of VIMS and sensory conflict from a modeling perspective. The apparatus and the navigation mechanism used in our experiments will be explained in Section 3. Section 4 will present the experiment setup and the test procedure. Section 5 will discuss the results of the experiments. Before concluding, we will give in Section 6 a mean for predicting VIMS in VR.

2. Theory of visually induced motion sickness (VIMS)

The conceptual Bayesian model, proposed by Oman [Oma90], of the cognitive process for the sensory conflict theory suggested by Reason and Brand [RB75] is shown in Figure 1.a. An exogenous (externally generated) motion stimulus enters the model and a sensory conflict is created as an output. The coefficients of the state equations ($\mathbf{A}$, $\hat{\mathbf{A}}$) for the body ($\mathbf{B}$, $\hat{\mathbf{B}}$) and the sense organ dynamics ($\mathbf{S}$, $\hat{\mathbf{S}}$) are embodied in this model. Figure 1.b details the mechanism of the central nervous system (CNS), which plays a preponderant role in body activities. The hatted variables of the state estimator with its matrices correspond to the neural stores of Reason's more qualitative model [Rea78]. The observer continuously estimates and predicts the body orientation, and corrects the posterior estimation with a Kalman gain $\mathbf{K}$. Then, it re-identifies the observer coefficients ($\hat{\mathbf{A}}$, $\hat{\mathbf{B}}$, $\hat{\mathbf{S}}$), re-calculates $\mathbf{K}$ and updates the control strategy ($\mathbf{C}$) for the next iteration (the CNS repeats this chain infinitely and non-stop). The sensory conflict vector $\mathbf{c}$ is obtained by subtracting the actual sensory from the expected input $\hat{\mathbf{S}}\hat{X}$. When the velocity of a displayed image goes above a certain limit, the conflict vector grows because vestibular data is missing, leading to sickness.

Human perception has been adjusted and trained in a real environment but observed objects and events in a VE look more artificial even though we try to coat the objects and scenes with high resolution patterns. VEs create more divergence in the human perception from the beginning of

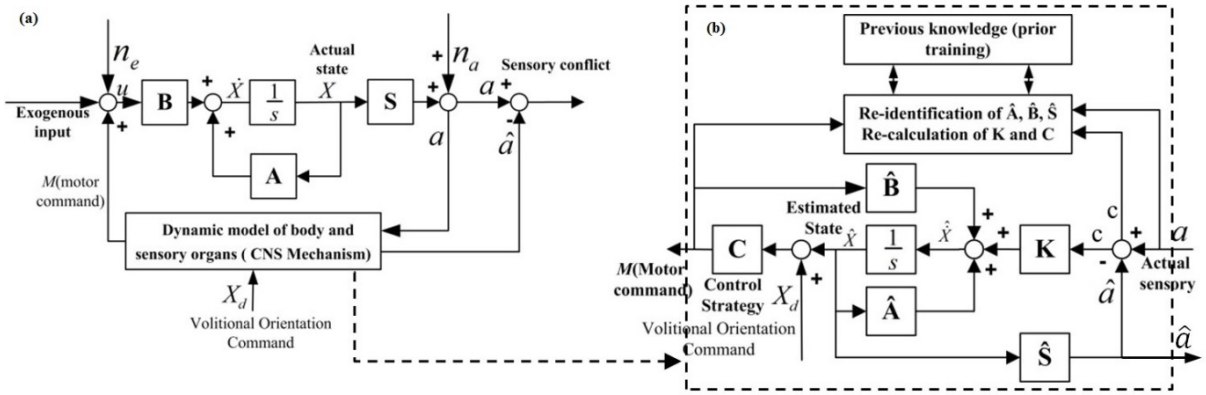

Figure 1: *a) Modified MS model proposed by Oman [Oma90] for the sensory conflict theory, b) dynamic model of the body, sensory organs and their signaling with the CNS.*

immersion, because of a visual-non vestibular (proprioceptive) conflict. This divergence increases the amplitude of the sensory conflict vector and leads to strong VIMS (the Kalman gain **K** and $\hat{\mathbf{S}}$ are overestimated or underestimated). VIMS in virtual environments mainly emerges due to visual-vestibular and visual-non vestibular conflicts. Since the first effect of the re-calculation error of **K** appears in the sensory-motor commands (after the control mechanism as seen in Figure 1.b), it can be easily sensed in the stance posture stability and the center of gravity sway area. This explains our choice of the center of gravity (COG) as a psychophysiological parameter for evaluating and predicting VIMS in our study.

3. Test equipment and navigation mechanism

3.1. Apparatus and devices

We conducted the experiments in a CAVE system, to fully immerse the participants. The CAVE system we used consists in four $3 \times 3 \times 3$m walls with a 1400×1050px resolution per wall, two projectors per wall for stereoscopic vision, with an infrared-based tracking system to track the user's location in the CAVE and in the VE.

A software development platform called iiVR was developed to manage the connection between the display projectors, the infrared cameras, the hardware resources and a network of navigation/interaction devices. It uses OpenSceneGraph on top of OpenGL to render 3D virtual scenes and incorporates the properties of the VE into the model. The generated model is projected at 60fps in the CAVE system via MPI and four NVidia Quadroplex GPUs. All the C++ functions were wrapped under Javascript functions to make the development faster and easier for programmers.

Navigation/interaction devices are connected via Virtual Reality Peripheral Network (VRPN) to iiVR. The overall latency is around 40ms.

A test platform was developed on a Java Virtual Machine (JVM) using MATLAB engine C++ library, to import test data from the experiments via VRPN and to analyze it easier and faster using MATLAB scripting language, Simulink and processing toolboxes.

For the measurements of the participants' COG, a Techno Concept sensor [Tec07] was used (see Figure 2). The sensor can measure left/right and forward/backward signals in real-time and calculate up to 13 parameters from the signals. Other sensors could be used such as the well-known Wii Fit board, however, the one we used was more accurate with more data outputs.

Figure 2: *COG sensor used during the experiments.*

3.2. Navigation mechanism

As we want to evaluate VIMS in a typical navigation task in a 3D immersive VE, we decided to use a so-called Flystick device as a navigation device. The Flystick has five buttons, one joy-stick handle, a laser-based optic tracker (position and orientation), and a trigger button. Figure 3 demonstrates the upper view of the Flystick.

The navigation task is initiated and terminated when the "start" and "stop" buttons are pressed respectively. The movement in the virtual scene can be accelerated/decelerated by two buttons allocated for this purpose on the Flystick (buttons sticked "+" and "-") as shown in Figure 3. The resolution of the changes of the movement speed is 0.45m.s^{-1}. The speed controller was designed to keep the user's speed within certain limits to ease navigation. When the user crosses the upper speed limit (6.5m.s^{-1}), the speed is decreased automatically to the baseline speed (here 2m.s^{-1}).

Forward movement is achieved by pushing the joy-stick handle forward (yellow handle in Figure 3). Rotation in the virtual scene is achieved by pushing the handle to the left or the right (first option), or by rotating the Flystick in the desired direction (second option). We restricted the possible movements in the virtual scene by allowing only forward movement and a rotation of up to $\pm 15^{\circ}$to the left and right, to avoid biases in the measurements.

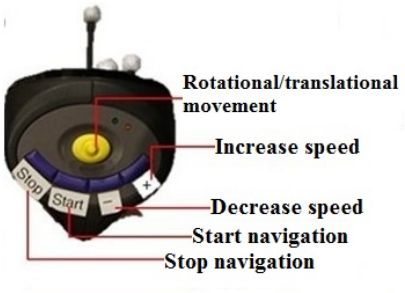

Figure 3: *Flystick and navigation sub-task assigned to each button.*

4. Experiments

In VR, different parameters are involved in VIMS, such as circular and linear vection, latency, foreground/background motion, field of view, image speed, frame rates, and so on. We choose to change the navigation velocity to ensure strong induction of VIMS during navigation while keeping the scene texture and the distance from the virtual scene constant for all the participants. Indeed, it is known that the speed has influence on sickness [SLA01]. This study focused only on translational movement.

4.1. Participants

Participants were asked to take part in two experiments. The first experiment, referred to as the "pre-test", was set up to select participants more resistant against VIMS, for the second experiment, referred to as the "main experiment", that was established to study the effect of independent parameters (navigation speed) on the level of VIMS. In the second experiment, we applied harder conditions (longer test period and faster speed), explaining the reason for the pre-test.

Seventeen subjects (13 males and 4 females: 31.58±12.69 years old, 74.65±15.22kg), called "Group 1", chosen from the members of the university, participated voluntarily (no compensation) in the first experiment, and nine male adults from Group 1 (26.33±3.81 years old, 76.33±16.34kg), called "Group 2", were selected to perform the second experiment. Group 2 did the test two weeks after the first experiment to ensure no effect from the first experiment would interfere with it. Enough information about the test procedure and possible risks before each experiment was provided individually. A pre-exposure general questionnaire (Q1) was obtained from each subject to know their backgrounds and to evaluate their health condition. The results of the questionnaire showed that there was no subject whose participation in the experiment would be unsuitable due to health issues.

4.2. Test procedure

Two rows of yellow balls, indicated by "Path 1", "Path 2", were lined up in parallel with a virtual wall, referred as the visual stimuli pattern (Figure 4.a). The distance between each line and the virtual wall were set to 2 and 4 meters, as shown and tagged by D_1 and D_2 in Figure 4.a. Figure 4.b shows the real setup.

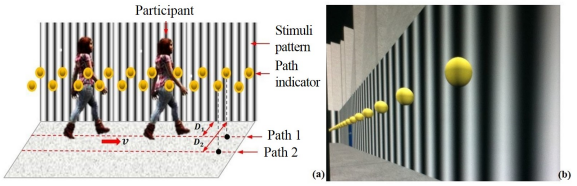

Figure 4: *a) Test parameters, path planning for navigation inside a 3D VE, b) navigation path set up inside a scale-one 3D immersive environment.*

4.3. First experiment (pre-test)

The pre-test was conducted in nine steps:

1. A pre-exposure questionnaire was asked to be filled out (Q1).
2. A training period was proposed for t_0 to get used to the navigation device before exposing the participants to the visual stimuli.
3. The COG for each participant was recorded for $t_1 = 30$s (pre-exposure measurement).
4. The participants navigated along path 1 (see Figure 4.a) for t_2s with a speed of 2m.s^{-1}.
5. The COG was recorded immediately after navigation for $t_3 = t_1$s.
6. A post-exposure questionnaire (Q2) was filled. The questionnaire we used was Kennedy's SSQ questionnaire [KLBL93] to calculate the sickness score.

7. The participants navigated along path 2 (see Figure 4.a) for t_2s with a speed of 2m.s^{-1}.
8. The COG was recorded immediately for t_3s.
9. Another SSQ was filled and the test terminated.

4.4. Second experiment (main experiment)

The participants navigated only along path 1 during the second experiment. This experiment took place in five steps. Because the conditions were harder, we could stop the experiment anytime if the participants would feel sick (we asked them to inform us if felt abnormal uneasiness in their stomach and head) or if the sickness scores reported by the participants changed abruptly (we did not have any case with severe sickness leading to vomiting or other symptoms during the experiment thanks to the pre-test but we put this condition only for precaution). The five steps were:

1. The COG for each participant was recorded for $t_0 = 30$s (pre-exposure measurement).
2. The participant navigated along path 1 (see Figure 4.a) for t_1s with a baseline speed of 2m.s^{-1}.
3. The COG was recorded for t_0s.
4. An SSQ was filled.
5. The navigation speed was increased of 0.45m.s^{-1} (see section 3.2).

Steps 2 through 5 were repeated 7 times for equal periods. The last measurement is referred as the post-exposure measurement.

5. Results and discussion

5.1. First experiment (pre-test)

The COG data from the first experiment (the pre-test) were analyzed to see clearly which parameter has underwent significant changes. 13 parameters of the COG sensor were extracted and averaged over all the participants for pre-exposure and post-exposure. The most influential parameters for the rest of the study can be identified only by looking at the variation of these values, i.e., the difference between the pre- and the post-exposures measurements.

From the statistical analysis for $n = 17$ participants, it comes out that 6 out of 13 COG parameters including Area ($F(1,16) = 198.6$, $p < 0.005$), Length ($F(1,16) = 154.9$, $p < 0.005$), Lng. L/R ($F(1,16) = 105.2$, $p < 0.001$), Lng. F/B ($F(1,16) = 149.5$, $p < 0.001$), Slope ($F(1,16) = 91.23$, $p < 0.01$), and S Var. ($F(1,16) = 98.23$, $p < 0.001$) (see Table 1) have undergone a significant variation. The other parameters either did not follow a specific trend or did not undergo significant variations. Therefore they have not been considered in the rest of this study.

If we recall that we hypothesized a change in the COG's area and shape as sickness occurred (H1), from Table 1, the Area parameter follows this trend.

5.2. Subject selection

We defined three susceptibility indexes for the selection of the participants allowed to do the main experiment:

- A sensitivity index (S) defined as the difference between the two post-exposure sickness scores resulting from the SSQs for each path divided by the exposure time:

$$S = \left| \frac{\mathrm{SSQ}_{\mathrm{path2}} - \mathrm{SSQ}_{\mathrm{path1}}}{t_2} \right| \quad (1)$$

- An average sickness index (AS):

$$AS = \frac{\mathrm{SSQ}_{\mathrm{path1}} + \mathrm{SSQ}_{\mathrm{path2}}}{2} \quad (2)$$

- An accumulative sickness index (ACS)

$$ACS = \mathrm{SSQ}_{\mathrm{path1}} + \mathrm{SSQ}_{\mathrm{path2}} \quad (3)$$

From these indexes, we defined two criteria to eliminate or allow a participant to continue the tests:

Criterion 1 if $AS > 50$ and $ACS > 90$, then the participant is considered as susceptible to strong VIMS (Criterion 1=1);
Criterion 2 if $S > 0.5$, then the participant is considered as susceptible to strong VIMS (Criterion 2=1);

A participant is eliminated from the second experiment if both criteria are equal to 1.

With these criteria, 4 female and 4 male were identified as susceptible subjects and got strongly sick during the first experiment (results from the SSQs ($AS = 95.74$, $ACS = 191.48$ and $S = 1.17$ in average) and from what they verbally mentioned). The rest of the participants were not strongly sick and were selected to participate in the second experiment. Based on the pre-test questionnaire (Q1), most of selected subjects were daily computer users and playing computer/digital games at least once a week.

5.3. Second experiment (main experiment)

The second experiment was carried out under harder conditions and a longer period ($t = 50 \pm 20$min, 3min in average to complete navigation per step) based on the test procedure explained in Section 4.4. We analyzed the experiment data in both the time and frequency domains to highlight some features for the estimation and prediction of VIMS.

5.3.1. Time domain analysis

Forward/Backward (F/B) and Left/Right (L/R) sway signals were recorded by the COG sensor at 8 points during the test (see Section 4.4). Figure 5 shows the F/B (in red color) and L/R (in blue color) signals for pre- and post-exposures for one participant. As seen, it is difficult to compare these two signals in the time representation without any feature extraction. We prefered thus calculating the evolution of the COG's area.

	COG SENSOR DATA				
PARAMETERS	abbreviation	pre-exposure	post-exposure	variation	p-value
Area (mm^2)	Area	29	553.4	524.4	0.0035
Locus length (mm)	Length	163	489.3	326.3	0.0023
Locus length of Left/Right (mm)	Lng. L/R	59.9	195.5	135.6	0.0001
Locus length of Forward/Backward (mm)	Lng. F/B	127.5	436.9	309.4	0.00054
Slope	Slope	43	129.3	86.3	0.0075
Speed Variance ($mm.s^{-1}$)	S Var.	10.7	188.1	177.4	0.00017

Table 1: *Significant features extracted from averaged pre- and post-exposures measurements of the COG sensor.*

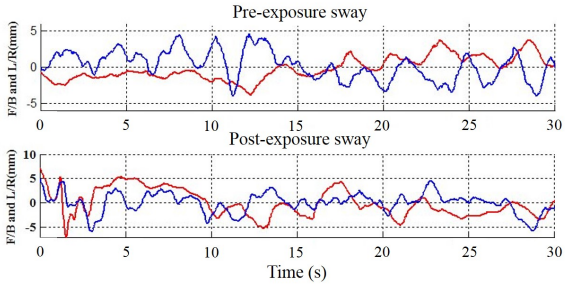

Figure 5: *Example of F/B and L/R sway signals for pre- and post-exposures for one participant.*

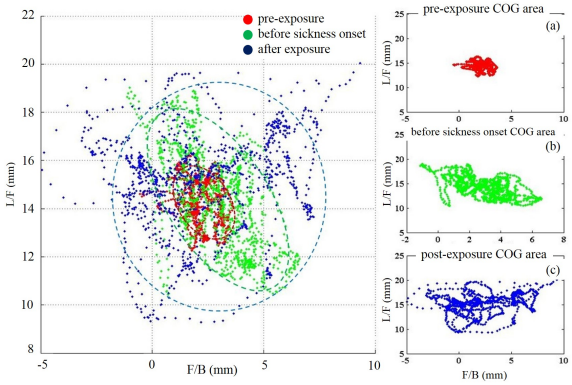

Figure 6: *Variation of the COG's area and shape: (a) pre-exposure, (b) at the sickness onset, (c) post-exposure.*

Though we measure a total of 8 points, only three instances are more important in this study: the baseline (at the beginning of the test, also called pre-exposure), at the sickness onset (just before sickness) and after sickness (at the end of the experiment, also called post-exposure). Though very little is known about the time of sickness onset, in our case, it will be defined as the moment where sudden change is observed between two consecutive SSQ scores (two consecutive measurements). This change can be calculated using the sensitivity index S defined in Section 5.2. For example, suppose, from the SSQ scores, $S = 8.3$ after the fourth navigation time and $S = 60$ after the fifth time, it means the sickness onset is at the fourth time as S highly increased.

The COG's areas associated with these three instances are depicted in Figure 6. On the right side of Figure 6, a zoom is made to show the area in each of the three instances: pre-exposure (Figure 6.a), at the sickness onset (Figure 6.b) and post-exposure (Figure 6.c). These areas are superimposed as a scatter plot to highlight the differences between each area. As seen, the post-exposure area distributed sparsely compared to the pre-exposure one. The COG's area is defined as the geometric shape (ellipse or circle) containing 90% of the points. The shape is almost circular in post-exposure (blue area in Figure 6), while it remains elliptical (red and green areas) till the sickness onset.

Figure 7 shows the variation of the area from the beginning to the end of the experiment at each measurement point. Two examples from the experiment are provided to explain how VIMS can be deduced from the variation of the geometric shape and the COG's area. In the first example, the area starts with an elliptical shape (Area=234.38mm^2), remains elliptical during 7 steps till the sickness onset (Area=423.13mm^2), while immediately after, it switches from an ellipse to a circle (Area=553.41mm^2). In the second example, the ellipse to circle alternation occurs in the fifth stage, however the dilation of the area continues till the end of the experiment. As a result, when sickness appears, the COG's area shape changes and dilates as sickness increases.

From the measurements and the calculation of the COG's area, statistical analysis showed a significant effect of the speed incremental variation on the area between post-exposure and pre-exposure (averaged SSQ score difference of 325.56, $F(1,8) = 133.86$, $p = 0.0015$). The same effect has been observed for the area's shape ($F(1,8) = 112.21$, $p = 0.0054$).

5.3.2. Frequency domain analysis

When the participant is not sick, his/her body remains in a stable state, meaning only voluntary movements of the body can occur. When the participant is subject to visual stimuli leading to sickness, as mentioned earlier, his/her body bal-

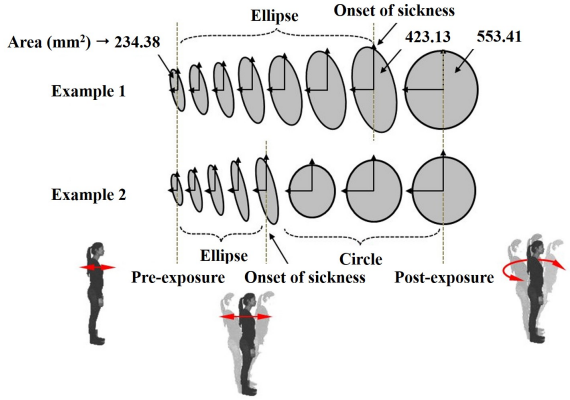

Figure 7: *Variation of the COG's area and shape during the eight steps of the experiment for two participants.*

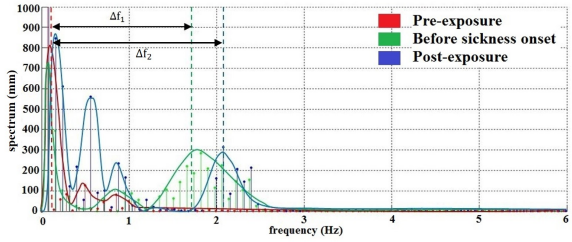

Figure 8: *Frequency components of the F/B sway signal for the same subject for pre-, post-exposures and at the sickness onset instances. Continuous curves represent curve fittings over the discrete values.*

ance malfunctions, resulting in involuntary movements. Bos showed that the switch between voluntary and involuntary movements can be set at 1Hz of the frequency of the body motion [Bos03]. Therefore we will study the spectrum of the sway signal to caracterize and predict the presence of VIMS.

The spectrum of the F/B sway signal (the L/R signal has the same characteristics) was calculated at the three moments: before sickness, at the sickness onset and after exposure, using FFT (see an example for the same participant in Figure 8). The spectrum of the movement can extend up to 20Hz, however for this subject example, the amplitude of the spectrum is almost close to zero for $f \geq 4$Hz. As seen in Figure 8, before exposure, the spectrum (in red color) has all its frequency components below 1Hz: 0.0-0.36Hz and 0.43-0.93Hz, meaning they are related to voluntary movement, i.e., no sickness. The spectrum associated with the sickness onset (in green color) has frequency components associated with voluntary movements (0.0-0.36Hz and 0.5-1.2Hz) and one component associated with involuntary movements (1.18-2.63Hz), according to Bos' theory, meaning the subject starts feeling VIMS. The post-exposure signal (in blue color) has components associated with voluntary movements (0.0-0.4Hz, 0.45-0.79Hz and 0.85-1.2Hz) and one component associated with involuntary movements (1.75-2.85Hz) which is further away from 1Hz compared to the one associated with involuntary movements at the sickness onset. Though several components are observed for voluntary movements, the first one (close to zero, marked with a vertical red dotted line in Figure 8) is the most significant one. Later, we will refer to voluntary and involuntary movement components as low frequency (LF) and high frequency (HF) components respectively.

We found significant differences across the subjects between the HF component at the sickness onset and the LF component of the pre-exposure spectrum (reference component), named Δf_1 in Figure 8 ($\Delta f = 1.80$Hz, $F(1,8) = 85.71$, $p = 0.0048$), as well as between the HF component at post-exposure and the LF component of the pre-exposure spectrum, named Δf_2 in Figure 8 ($\Delta f = 2.13$Hz, $F(1,8) = 98.21$, $p = 0.0048$). Especially, we observed that the HF component moves away as long as sickness increases. As a result, we can deduce that the difference between HF and LF components indicates the level of sickness: the more sickness the bigger the difference between these two components. Therefore (H2) was proven.

5.3.3. Subjective data analysis

The level of sickness for the nine participants was calculated using the SSQs at the sickness onset and post-exposure, assuming that the sickness level at pre-exposure was a natural zero (no stimuli) for healthy subjects. The statistical analysis on all SSQ scores showed that the level of sickness increased dramatically especially with an increase of the velocity (SSQ scores of 325.56 in average at post-exposure, $F(1,16) = 121.86$, $p < 0.042$).

5.4. Link with the theory of VIMS

In the presence of sickness, the body starts turning around its base in a circular shape. This is the consequence of a malfunction of the **C** function (control strategy of Figure 1). Based on our study, the frequency of this sway appears in the bandwidth 1.3-2.75Hz in average after exposure and can move to higher frequencies up to 20Hz. In particular we observed that for some participants, the HF component moved after 5Hz, resulting in severe sickness.

6. Prediction of VIMS

In the previous section, we found that the amount and the type of the COG's area dilation, and the difference between the LF and HF components of the sway signals provide information on the level of sickness. From these results, we can predict the onset of VIMS and track the level of sickness during a navigation task in a virtual environment. When the

level of sickness goes above a certain threshold, we can inform the user or stop the operation of the process. Figure 9 shows an example of the implementation of such prediction in a VR application using our method.

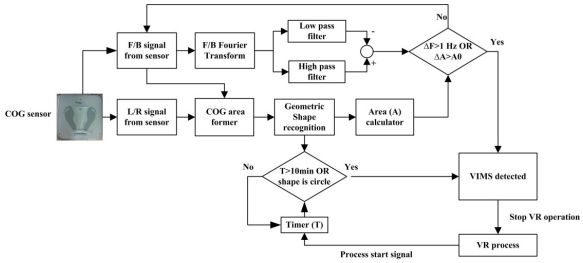

Figure 9: *VIMS prediction in a real-time VR application.*

7. Conclusion

We have proved that in a 3D virtual environment, when sickness appears, the area of the COG is dilated and the shape of the area tends to change from an ellipse to a circle. At the same time, we saw that the difference between LF and HF components of the COG's signals increases. Also a speed incremental variation has a significant effect on sickness. Both hypotheses were hence assessed.

Future work will investigate other features for predicting VIMS in a 3D virtual environment, and the effect of other parameters of a VR system on the level of VIMS.

Acknowledgements

This work was supported by the FUI Callisto grant.

References

[BBG08] BOS J. E., BLES W., GROEN E. L.: A theory on visually induced motion sickness. *Displays 29*, 2 (2008), 47–57. 2

[Ben88] BENSON A. J.: Spatial disorientation-general aspects. *Aviation Medicine 1* (1988), 405–433. 1

[Bos03] BOS J. E.: Method for the prevention of motion sickness, and apparatus for detecting and signaling potentially sickening motions, 2003. 7

[CHM91] CHEUNG B., HOWARD I., MONEY K.: Visually-induced sickness in normal and bilaterally labyrinthine-defective subjects. *Aviation, Space, and Environmental Medicine 1* (1991), 1–10. 1

[Cob99] COBB S.: Measurement of postural stability before and after immersion in a virtual environment. *Applied Ergonomics 30*, 1 (February 1999), 47–57. 2

[Irw81] IRWIN J.: The pathology of sea-sickness. *The Lancet 118*, 3039 (1881), 907–909. 1

[KGMB68] KENNEDY R. S., GRAYBIEL A., MCDONOUGH R. C., BECKWITH D.: Symptomatology under storm conditions in the north atlantic in control subjects and in persons with bilateral labyrinthine defects. *Acta oto-laryngologica 66*, 1-6 (1968), 533–540. 1

[KLBL93] KENNEDY R. S., LANE N. E., BERBAUM K. S., LILIENTHAL M. G.: Simulator sickness questionnaire: An enhanced method for quantifying simulator sickness. *The international Journal of Aviation Psychology 3*, 3 (1993), 203–220. 2, 4

[Kol95] KOLASINSKI E. M.: *Simulator Sickness in Virtual Environments*. Tech. Rep. 1027, U.S. Army Research Institute, 1995. 2

[KS96] KENNEDY R., STANNEY K.: Postural instability induced by virtual reality exposure: development of a certification protocol. *International Journal of Human-Computer Interaction 8*, 1 (1996), 25–47. 2

[Mon72] MONEY K.: Measurement of susceptibility to motion sickness. In *AGARD Conference Proceedings* (1972), pp. B2–1–B2–4. 1

[Oma90] OMAN C. M.: Motion sickness: a synthesis and evaluation of the sensory conflict theory. *Canadian Journal of Physiology and Pharmacology 68*, 2 (1990), 294–303. 2, 3

[OTS*95] OKAWA T., TOKITA T., SHIBATA Y., OGAWA T., MIYATA H.: Stabilometry. significance of locus length per unit area (l/a) in patients with equilibrium disturbances. *Equilibrium Research 55*, 3 (1995), 283–293. 2

[RB75] REASON J., BRAND J.: *Motion sickness*. Academic Press, London, 1975. 1, 2

[Rea78] REASON J.: Motion sickness adaptation: a neural mismatch model. *Journal of the Royal Society of Medicine 71*, 11 (1978), 819–829. 2

[SH98] STANNEY K. M., HASH P.: Locus of user-initiated control in virtual environments: Influences on cybersickness. *Presence: Teleoperators and Virtual Environments 7*, 5 (1998), 447–459. 1

[SHH*00] STOFFREGEN T. A., HETTINGER L. J., HAAS M. W., ROE M. M., SMART L. J.: Postural instability and motion sickness in a fixed-base flight simulator. *Human Factors: The Journal of the Human Factors and Ergonomics Society 42*, 3 (2000), 458–469. 2

[SLA01] SO R., LO W., ANDY T.: Effects of navigation speed on motion sickness caused by an immersive virtual environment. *Human Factors 43*, 3 (2001), 452–461. 4

[SSBP99] STOFFREGEN T. A., SMART L. J., BARDY B. G., PAGULAYAN R. J.: Postural stabilization of looking. *Journal of Experimental Psychology: Human Perception and Performance 25*, 6 (1999), 1641. 2

[SVBS07] SCIBORA L. M., VILLARD S., BARDY B., STOFFREGEN T. A.: Wider stance reduces body sway and motion sickness. In *Proc. VIMS* (2007), pp. 18–23. 2

[Tah09] TAHBOUB K. A.: Biologically-inspired humanoid postural control. *Journal of Physiology-Paris 103*, 3 (2009), 195–210. 2

[Tec07] TECHNOCONCEPT: *Techno-concept balance board manual, Notice Logiciel SabotSoft*, 2007. 3

[TFMM07] TAKADA H., FUJIKAKE K., MIYAO M., MATSUURA Y.: Indices to detect visually induced motion sickness using stabilometry. In *First International Symposium on Visually Induced Motion Sickness, Fatigue, and Photosensitive Epileptic Seizures (VIMS2007)* (2007), vol. 1, pp. 178–183. 2

[YAM*05] YOKOTA Y., AOKI M., MIZUTA K., ITO Y., ISU N.: Motion sickness susceptibility associated with visually induced postural instability and cardiac autonomic responses in healthy subjects. *Acta oto-laryngologica 125*, 3 (2005), 280–285. 2